Full Length Article

Ag-Mo modified SCR catalyst for a co-beneficial oxidation of elemental mercury at wide temperature range

Songjian Zhao [a,b], Haomiao Xu [a], Jian Mei [a], Yongpeng Ma [c], Tong Lou [a], Zan Qu [a], Naiqiang Yan [a,*]

[a] School of Environmental Science and Engineering, Shanghai Jiao Tong University, 800 Dong Chuan Road, Shanghai 200240, PR China
[b] School of Chemistry and Chemical Engineering, Shanghai Jiao Tong University, 800 Dong Chuan Road, Shanghai 200240, PR China
[c] Henan Collaborative Innovation Center of Environmental Pollution Control and Ecological Restoration, Zhengzhou University of Light Industry, No. 136, Science Avenue, Zhengzhou 450001, PR China

HIGHLIGHTS

- V-Mo-Ti was more active than V-W-Ti for the catalytic oxidation of elemental mercury.
- The dope of Ag can improve markedly the mercury oxidation efficiency of V-Mo-Ti.
- The catalytic mechanisms were different at various temperature ranges.

GRAPHICAL ABSTRACT
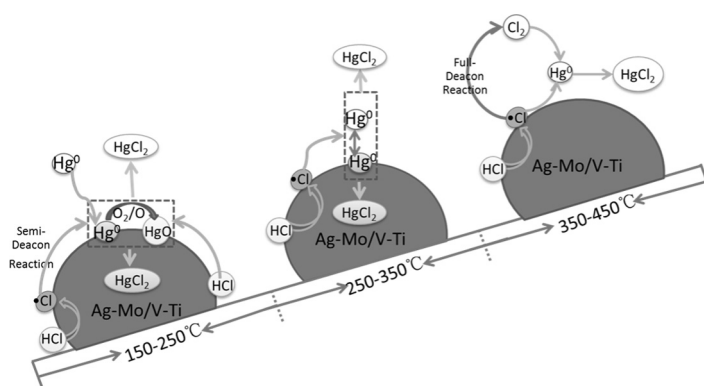
ARTICLE INFO

ABSTRACT

V_2O_5-MoO_3-TiO_2 (V-Mo-Ti) is often used as a selective catalytic reduction catalyst for NOx from coal-fired flue gas. The performance of a V-Mo-Ti catalyst for the oxidation of elemental mercury (Hg^0) was investigated. It was found that Mo was resistant toward sulfur dioxide and can enhance the Hg^0 adsorption capacity. Ag was employed to enhance the Hg^0 oxidation reaction and can enlarge reaction temperature window. Doping with Ag can significantly enhance the oxidation of Hg^0, and adding only 0.5% Ag can keep Hg^0 oxidation efficiency to approximately 90% with 5 ppm HCl, with an increase of 20–40% compared to that of V-Mo-Ti catalyst. Besides, the reaction temperature window of catalyst was enlarged from 150 to 400 °C. TEM and XPS characterization data indicated that Ag nanoparticles were loaded on the Mo/V-Ti carrier, maintaining Ag-Mo/V-Ti at a higher oxidation state. Furthermore, the TPR and Deacon reaction tests suggested that the Ag dopant might enhance the redox behavior, which facilitates the Deacon or semi-Deacon reactions for HCl activation. In addition, Hg^0 desorption and breakthrough experiments and mercury valence state change experiments were carried out to investigate the Hg^0 catalytic oxidation mechanisms at various temperature ranges.

© 2017 Elsevier Ltd. All rights reserved.

1. Introduction

Mercury (Hg) in coal-fired flue gas is a major concern due to its volatility, persistence, and bioaccumulation [1]. This substance has

* Corresponding author.
  E-mail address: nqyan@sjtu.edu.cn (N. Yan).

been listed as a hazardous and toxic pollutant under Title III of the 1990 Clean Air Act Amendments (CAAA) in United States [2]. Recently, the U.S. EPA developed federal standards to limit toxic gas emissions (including mercury) from power plants in December 2011 [3]. Besides, in October 2013, a new international convention to control mercury emissions, which was named the Minamata Convention on Mercury, was signed by most countries in response to global mercury pollution problem [4]. As one of the largest mercury emission countries in the world, China has also paid increasing attention to mercury control. In addition, the latest issued "Emission Standard of Air Pollutants for Thermal Power Plants" (GB13223-2011) had been signed in 2015 [5].

Mercury from coal-fired flue gas exists in three forms: elemental mercury (Hg^0), oxidized mercury (Hg^{2+}) and particulate-bound mercury (Hg^p) [4]. Hg^p attached to fly ash can be captured by particulate control devices, such as electrostatic precipitators (ESP) and fabric filters (FF) [5]. Hg^{2+} is water-soluble and can therefore be effectively removed by a wet flue gas desulfurization (WFGD) system [6]. However, Hg^0 is difficult to remove from the flue gas due to its high volatility and low solubility in water. An efficiency method for Hg^0 removal is catalytic oxidation process, in which convert Hg^0 to Hg^{2+}. The oxidized mercury can be subsequently captured by the existing air pollution control devices.

Two major categories of catalysts for Hg^0 oxidation have been studied, the one is selective catalytic reduction (SCR) catalyst and the other one is metal oxide catalyst [7]. The catalysts used for SCR of de-NOx are also effective for mercury oxidation [8–10]. Controlling Hg with the existing air pollution control devices can reduce costs, which currently are the most selected methods for mercury control in a coal-fired power plant [11].

SCR catalysts consist of vanadia and tungsten oxides or molybdenum oxide on a titania support. Molybdena-vanadia SCR catalyst has a higher activity than vanadia alone [10], as well as more resistant toward arsenic poisoning [12]. In addition, molybdenum is frequently added to vanadium-based catalysts to enhance the catalytic performance toward various hydrocarbon oxidations, such as selective oxidations of benzene and toluene[13]. Bertinchamps et al. reported that VO_x-MoO_x/TiO_2 materials were the most active catalysts during a chlorobenzene oxidation compared to VO_x/TiO_2, VO_x-WO_x/TiO_2 and VO_x-MoO_x/TiO_2 [14]. However, a V-Mo-Ti SCR catalyst for Hg^0 oxidation was not examizied.

In general, the efficiency of Hg^0 oxidation over a SCR catalysts highly depend on HCl concentration of the flue gas [15]. However, the concentration of chlorine in most coals is often low in China, which affects the Hg^0 oxidation efficiency. Therefore, enhancing the Hg^0 oxidation catalytic activity from coal combustion flue gas with low HCl concentrations is essential. Historically, Ag nanoparticle has been recognized as an efficient catalyst in various reactions [16–18]. Ag can generate electrophilic oxygen [19], adding Ag to an SCR catalyst can promote the reaction. Ge et al. reported that after adding elemental Ag to vanadic oxide, the V=O bond strength was weakened and the activation energies for the desorption of surface oxygen species significantly decreased [20]. Ag can also be used as an adsorbent to remove Hg^0 at low temperatures through an amalgamation mechanism. Yuan et al. used Ag_2O-doped TiO_2 for Hg^0 removal with an approximately 95% due to the formation of a silver amalgam [21]. Dong et al. [22] prepared magnetic zeolite composites with supported silver nanoparticles as sorbents; this material could completely capture mercury at temperatures up to 200 °C. However, Ag has not been used as an active catalyst for Hg^0 oxidations instead of adsorption in the presence of HCl up to now.

In this study, catalysts were prepared using a room-temperature impregnation method. The physical and chemical properties of the catalysts, as well as the Hg^0 oxidation efficiency of the Ag-Mo modified SCR catalyst at low HCl concentrations,

were investigated. Meanwhile, the effects of the flue gas components on the Hg^0 oxidation were also examined. Furthermore, the catalytic mechanisms involved in improving the efficiency at various temperatures were discussed.

2. Experimental

2.1. Preparation of catalysts

Please refer to Material preparation Methods in the Supporting Information.

2.2. Catalytic activity evaluation

The catalytic activity was evaluated in a simulated gas preparation system and a catalytic reactor. A cold vapor atomic absorption spectrometer (CVAAS) and an online data acquisition system were employed for Hg^0 detection. The simulative gas formulating system and catalytic reactor included eight mass flow controllers to prepare simulated flue gas compositions and a fixed-bed reactor (a quartz tube with a 6 mm inner diameter, and a tube-type resistance furnace). The catalyst (40–60 mesh particles, with a bulk volume of 0.141 mL) was added to a quartz tube with quartz wool to avoid loss. Hg^0 vapor was prepared from the Hg^0 permeation tube and was blended with the gases before they entered the reactor. The concentration of Hg^0 in the simulated gas was analyzed using a mercury analyzer (CVAAS SG-921).

At the beginning of each test, the gas containing the Hg^0 vapor was first bypassed without a catalyst and subsequently sent to the CVAAS to determine the baseline. When the concentration of Hg^0 remained within ±5% for longer than 30 min, the gas was diverted to the fixed-bed reactor with catalysts. 5 ppm HCl was passed to estimate the oxidation efficiency of Hg^0 until the catalysts were saturated. The gas flow rate was 30 L/h, corresponding to a space velocity (SV) of 2.13×10^5 h^{-1}. N_2 was used as the carrier gas, and the O_2 content was 4%. Because the catalysts were first saturated in 300 µg/m^3 Hg^0 plus N_2 and O_2 gas flow, the decrease of Hg^0 concentration across the catalysts after passing HCl was attributed to Hg^0 oxidation. Accordingly, the definition of Hg^0 oxidation efficiency (Eoxi) over catalysts is as follows:

$$\text{Eoxi } (\%) = \frac{\Delta Hg^0}{Hg_{in}^0} = \frac{Hg_{in}^0 - Hg_{out}^0}{Hg_{in}^0}$$

The valence state change for mercury was analyzed by Online Mercury Emissions Monitoring System (3300 RS).

Temperature programmed desorption curves of Hg proceeded as follows: a known amount of adsorbents were placed in adsorption device with N_2 + 4% O_2 at 30 L/h and 100 °C to adsorb mercury for 2 h; afterwards, the oxygen was stopped, and the Hg signal curve was recorded at 2 °C/min until 450 °C under nitrogen.

3. Results and discussion

3.1. Comparison of the Hg^0 catalytic oxidation efficiencies over various catalysts

To obtain a higher efficiency catalyst for oxidizing Hg^0 with low HCl concentration, the performances of prepared catalysts are investigated. Fig. 1 shows the Hg^0 catalytic oxidation efficiencies over various catalysts at 200 and 350 °C. V-Ti, Ag-Ti and Mo-Ti materials all showed low activity toward Hg^0 oxidation compared with TiO_2. When combining these components, the catalytic activity improved significantly due to the synergy between the V and Mo or Ag. In addition, V-Ti and Ag-Ti materials performed poorly when SO_2 was present, but the catalytic efficiency of Mo-Ti was
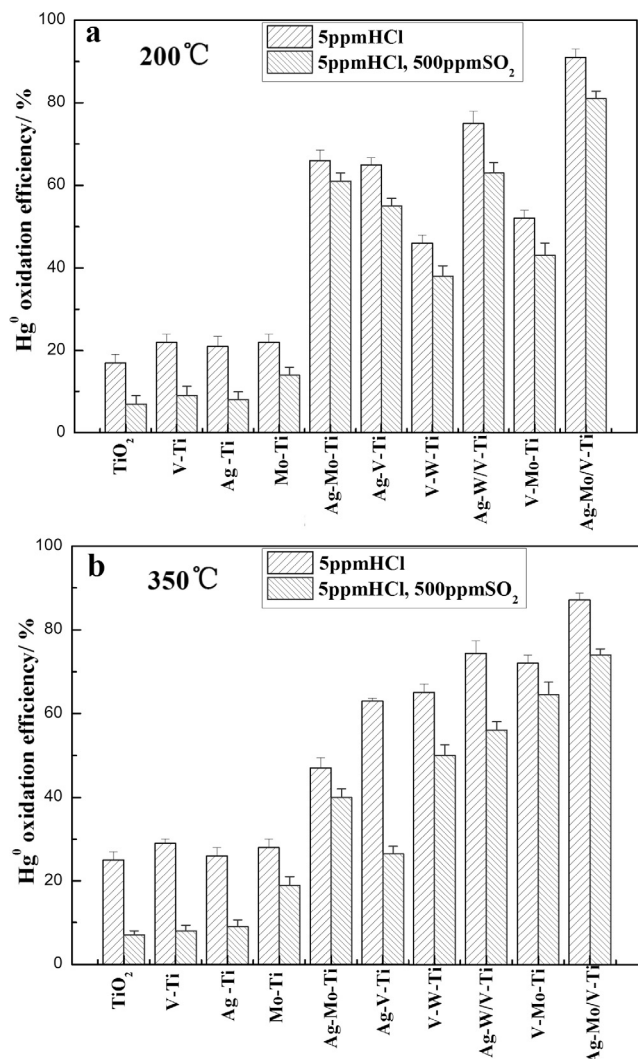
Fig. 1. Comparison of the Hg^0 catalytic oxidation efficiencies over various catalysts with 5 ppm HCl and the a mixture of 5 ppm HCl and 500 ppm SO_2 at 200 °C (a), 350 °C (b).

less affected. Therefore, Mo was resistant toward SO_2. The catalytic performances of the SCR catalysts (V-W-Ti and V-Mo-Ti) were both worse at low temperatures than that of at high temperatures, indicating that the SCR catalysts preferred high temperatures for the oxidation of mercury. However, V-Mo-Ti performed slight better than V-W-Ti at various temperatures. Therefore, V-Mo-Ti catalyst was selected for further modification with Ag. The performances of V-Ti, Mo-Ti, V-W-Ti and V-Mo-Ti were improved after adding Ag, indicating that Ag improved the oxidative abilities of the catalyst. Ag-Mo/V-Ti had the highest catalytic efficiency at both 200 and 350 °C, indicating that this composite is an excellent catalyst. This catalyst was also demonstrated a superior resistance toward SO_2. Therefore, the physical and chemical properties of the catalysts and the reaction mechanism should be discussed.

3.2. Catalyst characterization

To obtain the microscopic morphologies and structural information, transmission electron microscopy (TEM) analyses of as-prepared V-Mo-Ti and Ag-Mo/V-Ti nanoparticles were performed, as shown in Fig. 2.

Fig. 2(a) and (b) show that the V-Mo-Ti nanoparticles were crystalline and have a size of 20 and 40 nm. The existence of V and Mo

on the carrier can be proved by EDS analysis (Table S1). However, it could not be observed on the surface of the support. Therefore, vanadium and the molybdenum might be well dispersed on the TiO_2 surface. Fig. 2(b) shows the HRTEM images of V-Mo-Ti. The crystal lattice has a distance of 0.352 nm which can be assigned to anatase TiO_2 (1 0 1) [23]. Some small particles were attached to TiO_2 surfaces in Fig. 2(c) and (d); these particles were Ag nanoparticles. The HRTEM images in Fig. 2(d) corresponding to the circled areas in Fig. 2(c), in which the crystal lattices had distances of 0.235 nm, were attributed to cubic Ag (1 1 1) species [23].

The surface elements and their mass ratios in the V-Mo-Ti and Ag-Mo/V-Ti obtained via XPS are listed in Table S2. These values are consistent with the atomic contents utilized in an impregnation method.

Fig. S2 shows the XPS spectra of V-Mo-Ti and Ag-Mo/V-Ti over the spectral regions of Mo 3d, Ti 2p, O 1s, Ag 3d and V 2p. Fig. S2(a) shows three Mo 3d peaks. The peaks located at approximately 232.9 and 236.0 eV were attributed to the Mo 3d5/2 and Mo 3d3/2 electronic states of Mo^{6+}, respectively. While the peak at 231.1 eV was attributed to the Mo^{5+} in TiO_2 lattice [24]. However, only two peaks were located at approximately 232.9 and 236.0 eV in Fig. S2(b), which indicated that Mo was existed in Mo^{6+} by adding Ag.

Two typical Ti 2p peaks in Fig. S2(c) and (d) located at approximately 458.56 eV and 464.24 eV can be assigned to Ti^{4+} 2p3/2 and Ti^{4+} 2p1/2, respectively. However, an additional peak at 457 eV was detected that matched the trivalent state of titanium, as shown in Fig. S2(c) [25]. Therefore, the surface-deposited Ag could induce a change in the Mo and Ti chemical states, maintaining the higher oxidation states of Mo and Ti.

The O 1s XPS spectrum in Fig. S2(e) is asymmetric and comprised of many peaks. The peak at 531.8 eV can be related to hydroxyl oxygen [25]. The peak at 530.4 eV can be attributed to the chemical bonding of oxygen, which might be composed of different species, such as Ti—O, Mo—O and V—O bonds [25,26]. The binding energy of 528.2 eV was the characteristic peak for the atomically adsorbed "ionic" oxygen [27,28]. However, such peak was not observed in Fig. S2(f). Therefore, the O 1s peak at 528.2 eV denoted a nucleophilic state, while the peak at 530.4 eV denoted an electrophilic state [29]. The electrophilic oxygen can improve the oxidation step by converting the low valence states to high valence states for metal ions, proving that the high oxidation ability of catalyst was imparted after adding silver.

The Ag 3d5/2 binding energies for Ag, Ag_2O and AgO were 368.4, 367.7, and 367.4 eV, respectively [25]. The XPS peak for Ag-Mo/V-Ti in Fig. S2(g) clearly shows that Ag present in a mixture state of metallic silver (Ag^0) and Ag^+ (Ag_2O) in which the metallic state was dominant. The V 3d XPS spectrum in Fig. S2(h) is weak due to the low vanadium content. Therefore, the vanadium existed in a high state due to the electrophilic properties of silver, improving the oxidation of V^{4+} to V^{5+} in the Mars and Van Krevelen mechanism and therefore facilitating the catalytic reaction [19].

The TPR profiles of the as-prepared catalysts are shown in Fig. S3. As observed in Fig. S3(a), a broad reduction peak was present starting from 100 °C and centered at 150 °C, in which could be attributed to the reduction peak of Ag_2O on the support [30].

Fig. S3(b) shows two reduction peaks. The peak at approximately 150 °C was related to the reduction of Ag_2O referred to in Fig. S3(a). The peak at approximately 260 °C was assigned to the reduction peak for the dispersed vanadium oxide, which was shifted to a lower temperature relative to V-Ti in Fig. S3(c). The activation energy values for the desorption of the surface oxygen species (O^- and O^{2-}) might have decreased significantly after adding silver [20,30].

The reduction peak at approximately 450 °C in Fig. S3(c) can be attributed to the typical reduction peak for dispersed vanadium
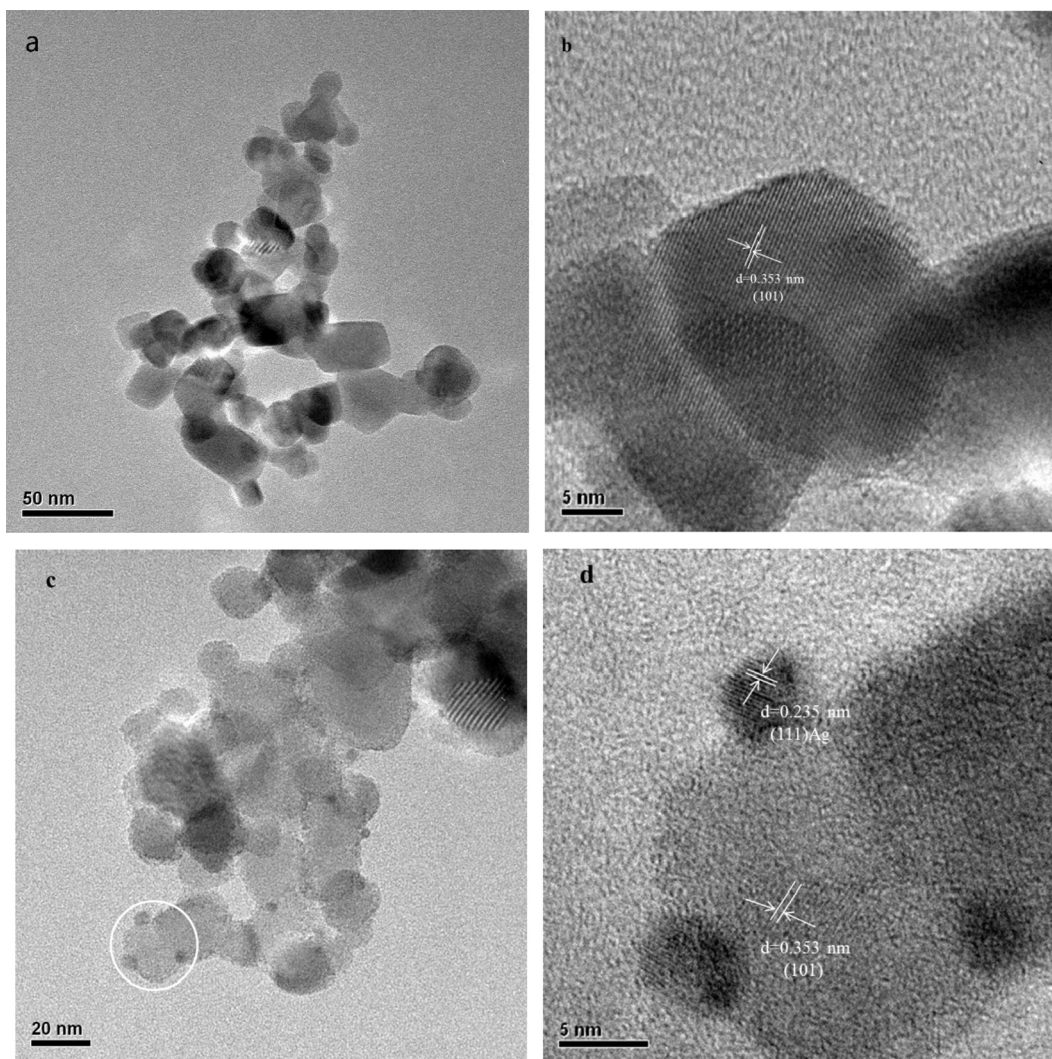
Fig. 2. TEM and HRTEM images of the V-Mo-Ti (a, b) and Ag-Mo/V-Ti(c, d).

oxide [31]. This peak's temperature was lower than the reduction peak for bulk vanadium oxide, which includes four peaks (678 °C, 728 °C, 856 °C, and 982 °C) that correspond to the following sequential reductions: $V_2O_5 \rightarrow V_6O_{13} \rightarrow V_2O_4 \rightarrow V_6O_{11} \rightarrow V_2O_3$ [32].

The reduction profile for the V-Mo-Ti in Fig. S3(d) exhibits two peaks: the first peak (460 °C) was attributed to the simultaneous reduction of Mo^{6+} and V^{5+} in the V-Mo-O structures, forming Mo^{4+} and V^{3+}, covering a broad temperature range and indicating that the vanadium oxide and the molybdenum oxide species were highly dispersed on the support. The peak at 780 °C reflected the reduction of Mo^{4+} to Mo^0 [33].

The peak for Ag-Mo/V-Ti appeared at 180 °C in Fig. S3(e) was attributed to the reduction of Ag_2O; this signal trended toward higher temperatures after adding molybdenum, as shown in Fig. S3(b). It suggested that there was an interaction between Ag_2O and V-Mo-Ti, which made Ag_2O particles well dispersed on the support and reduced difficultly. The peaks for dispersed vanadium and molybdenum oxide species, as shown in Fig. S3(d), shifted toward lower temperatures due to the weaken of V=O and Mo=O bond strengths, resulted in the decreasing activation energy values for the desorption of surface oxygen species [20]. Such results were further proved by O_2-TPD analysis, shown in Fig. S4, in which the amount of desorption oxygen for

Ag-Mo/V-Ti was more than that of V-Mo-Ti, manifesting the adding silver was beneficial for the oxygen activation and adsorption.

3.3. Catalysts activity

Fig. S5 reveals Hg^0 catalytic oxidation efficiencies of the V-Mo-Ti and Ag-Mo/V-Ti with 5 ppm HCl at different temperatures. Fig. S5 shows that the catalytic activity of V-Mo-Ti increased initially before decreasing as the temperature increased. Therefore, the suitable temperature range for the V-Mo-Ti catalyst was 300–400 °C. The catalytic activity of Ag-Mo/V-Ti was high at all temperatures, reaching beyond 85% and revealing the broad temperature range of this catalyst, indicated that the redox temperature of the catalyst was decreased and the oxidative ability of the catalyst was improved after adding silver.

The Hg^0 catalytic oxidation efficiencies of Ag-Mo/V-Ti with various cases are shown in Fig. S6. The catalytic efficiency was high in the presence of HCl, decreasing initially before increasing slightly and finally decreasing as the temperature increased. The silver amalgam might have formed at low temperature, and the amalgamated Hg^0 interacted with the HCl in the flue gas stream to form a Hg-chloride intermediate before forming $HgCl_2$ [34]. In addition, the redox temperature of the catalyst decreased and the oxidation abilities of V, Mo improved after adding Ag. When the temperature

increased, the captured mercury could be released, slightly decreasing the catalytic efficiency [35]. Up to 350 °C, the oxidative ability of the catalyst increased because the catalytic activity of the SCR catalyst was higher at 350 °C than that at lower temperatures. The efficiency began to decline above 400 °C, indicating that excessively high temperatures decreased the catalytic activity. When SO_2 was added, the catalytic efficiency began to decrease at all temperatures, indicating that SO_2 competed for the active sites [36] or inhibited the Cl_2 formation [37]. The efficiency improves when adding nitric oxide, remaining consistent with the previous researches [36,38]. The effect of water was slight, as shown in Fig. S6, and the catalytic efficiency was inhibited slightly at low temperatures, consisted with some reports [36]. While increasing slightly at higher temperatures, which might be that some deactivation site of catalyst was reactivated by sweeping of water at high temperature.

3.4. Reaction mechanism analysis

To investigate the mercury combination property of catalysts, the Hg^0 desorption experiment is performed. Fig. 3 shows the Hg-TPD curves for the different catalysts. Fig. 3(a) shows that little Hg^0 desorption occurred when increasing temperature, revealing that the Hg^0 adsorption of V-Ti was very weak. When Mo was added, the adsorption of Hg^0 improved significantly, enabling reaction with the adsorbed Cl and enhancing the oxidation efficiency for Hg^0. The desorption temperature for V-Mo-Ti was high, meaning that the chemical bond between Hg and Mo was stronger. Two desorption peaks were observed for Ag-Mo/V-Ti. The peak at 175 °C could be attributed to the silver amalgam, decomposing Hg^0 and metallic silver metal as the temperature increased. Therefore, the silver adsorbed Hg at low temperatures before reacting with the adsorbed HCl, proving the excellent catalytic effect at low temperatures occurred as discussed above. The peak at approximately 225 °C was assigned to the Mo-Hg referenced in Fig. 3(b); This species benefitted the Hg^0 oxidization at moderate temperatures. Besides, it could find that there little adsorbed Hg^0 on the surface of Ag-Mo/V-Ti catalyst above 325 °C. In comparison, Ag-Mo/V-Ti exhibited a wide range of Hg^0 adsorption, improving the catalytic performance.

To clarify the influence factor of Hg^0 removal, the Hg^0 breakthrough experiments were conducted. Fig. S7 shows the Hg^0 breakthrough curves of Ag-Mo/V-Ti at various cases. It can be seen from the Fig. S7(a), the Hg^0 adsorption capacity of the

catalyst was gradually reduced with the increasing temperatures under anaerobic condition. And there were little adsorbed Hg^0 above 250 °C. After O_2 was added, the Hg^0 concentration was reduced, which indicated that Hg^0 could be oxidized by the catalyst of Ag-Mo/V-Ti under oxygen condition, and the activity of the catalyst was better at low temperature.

Fig. S7(c) shows the Hg^0 breakthrough curves over HCl pretreated Ag-Mo/V-Ti. It can be seen from the Fig. S7(c), when HCl was pretreated, the catalyst had high Hg^0 oxidation efficiency, and it was higher at low temperature than that at high temperature. Because the catalyst was purged by N_2 after HCl was pretreated. It had hardly Cl_2 adsorbed on the catalyst. And the component adsorbed on the surface of catalyst could be the active chlorine species formed by the reaction between HCl and Ag-Mo/V-Ti, which could be reacted with Hg^0. The amount of active chlorine species on the catalyst would decrease with the increasing temperature, and there were little active chlorine species adsorbed on the catalyst above 350 °C.

To determine the catalytic mechanism of the Hg^0 conversion over Ag-Mo/V-Ti, the yield experiment of Cl_2 was carried out.

Fig. S8 shows the Cl_2 produced by the Deacon Reaction. Fig. S8 (a) indicated that the yield Cl_2 was low at low temperatures, while it was increased as the temperature increased. In contrast with Figs. S5 and S6, the catalytic mechanism for Hg^0 oxidation was different at low and high temperatures. The low Cl_2 yield at low temperatures indicated that less atomic chlorine was available to form Cl_2 or that the atomic chlorines were adsorbed on active sites of the support at low temperatures. The Hg^0 oxidation by HCl over Vanadia-based SCR catalysts was reported to occur through the Eley-Rideal mechanism. The gas-phase or weakly adsorbed Hg^0 reacted with the adsorbed active Cl species [4]. The catalytic Hg^0 oxidation efficiencies for V-Mo-Ti in Fig. S5 were lower than those of Ag-Mo/V-Ti at low temperatures. Therefore, the adsorbed Cl reacted with the Hg^0 adsorbed on the support and silver amalgam in Ag-Mo/V-Ti followed the Langmuir-Hinshelwood mechanism. Ag could adsorb the Hg^0 to form the silver amalgam, increasing the amount of adsorbed Hg^0 When increasing the temperature, the adsorbed Hg^0 was converted to gas-phase Hg^0, inhibiting the amalgamation effect. At 350 °C, the production of active chlorine atoms increased, enabling reactions with the gaseous mercury. If the temperatures continued to rise, the adsorbed chlorine atoms were released from the surface of the catalyst to react with Hg^0 via direct gas phase oxidation. The activation energy for oxidizing Hg^0 over the catalyst was lower than the direct gas phase oxidation,
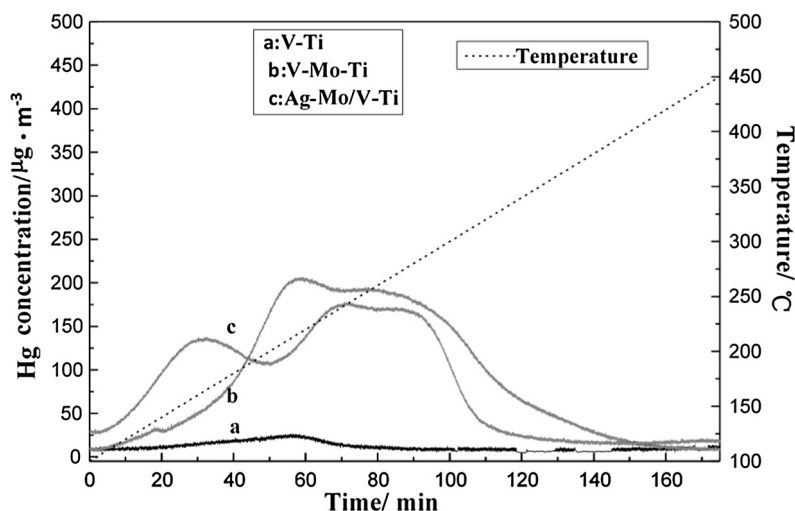
Fig. 3. Hg-TPD curves for the different catalysts: V-Ti (a), V-Mo-Ti (b), Ag-Mo/V-Ti (c).

decreasing the catalytic efficiency. The capacity for chlorine production strengthened when increasing the temperature because additional gaseous chlorine atoms were present or because the chlorine atoms had a higher activity, enabling reactions with the nearby chlorine atoms on the support.

Fig. S8(b) compares the Cl_2 yields of various catalysts, revealing that the Cl_2 yield increased when adding molybdenum. Therefore, the strong synergistic effect between Mo, V and Ti increased the catalytic performance. In addition, the Cl_2 yield increased further after adding silver, indicating that adding silver could improve the specific activation of Deacon Reaction, so that the oxidative ability of the catalyst was enhanced.

To further prove the results as-mentioned, the valence state change for mercury was analyzed. Fig. 4 shows the mercury concentration change curves at 150 and 350 °C. It can be seen from the Fig. 4(a) that the concentration of total mercury and Hg^0 both reduced when the flue gas through the catalyst. The concentration of Hg^0 was lower than that of total mercury. It indicated the Ag-Mo/V-Ti has an adsorption ability of Hg^0 at low temperature, and Hg^0 could be oxidized by the adsorbed oxygen or lattice oxygen of Ag-Mo/V-Ti. However, it hardly adsorbed Hg^0 at high temperature shown in Fig. 4(b), and Hg^0 was less oxidized. When oxygen was added, the mercury concentration continued to reduce both at low and high temperatures. More amount of Hg^{2+} was generated at low temperature than that of at high temperature, manifesting the oxidation ability of Ag-Mo/V-Ti was higher under oxygen condition at low temperature. After HCl was added, the Hg^0 removal efficiency was both further increased at 150 and 350 °C. Because Cl_2 was hardly produced at low temperature, the decreasing

concentration of Hg^0 was might that Hg^0 was reacted with adsorbed active Cl species to produce $HgCl_2$. Besides, the generated HgO would also react with HCl. The concentration of total mercury was reduced, which was might be that some amount of $HgCl_2$ was adsorbed on the catalyst. The Hg^0 could be oxidized by Cl_2 at high temperature due to the high Cl_2 yield referred to Fig. S8.

Based on the above analysis, the main reaction process for the Hg^0 oxidation over Ag-Mo/V-Ti at various temperature ranges can be showed in the Fig. 5.

It can be observed from the Fig. 5 that Hg^0 was adsorbed by Ag to form the silver amalgam or combined with Mo in the way of Mo-Hg at low temperate range (approximately 150–250 °C). And then reacted with the active chlorine species formed by the reaction between HCl and Ag-Mo/V-Ti to form a Hg-chloride intermediate before forming $HgCl_2$, which was named Semi-Deacon Reaction. $HgCl_2$ existed mainly on the surface of catalyst, while some would pass into flue gas due to the purge of high space velocity airflow. In addition, Hg^0 could be oxidized by oxygen or active oxygen through Ag-Mo/V-Ti, and the generated HgO would react with HCl. At about 250–350 °C, the captured mercury would be released. And the adsorbed Hg^0 and gaseous Hg^0 could react with the active chlorine species. With an increasing temperature, there was little adsorbed Hg^0 on the surface of Ag-Mo/V-Ti catalyst. And the active chlorine species began to form Cl_2 to react with gaseous Hg^0, which was named Full-Deacon Reaction. The mainly primary reaction pathway can be written as follows:

$$Hg_{(ad)} + Cl_{(ad)} \rightarrow HgCl_{(ad)} \tag{1}$$

$$Hg_{(g)} + Cl_{(ad)} \rightarrow HgCl_{(ad)} \tag{2}$$

$$HgCl_{(ad)} + Cl_{(ad)} \rightarrow HgCl_{2(ad)} \tag{3}$$

$$Hg_{(ad)} + O \rightarrow HgO_{(ad)} \tag{4}$$

$$HgO_{(ad)} + 2HCl_{(ad)} \rightarrow H_2O + HgCl_{2(ad)} \tag{5}$$

$$Cl_{(ad)} + Cl_{(ad)} \rightarrow Cl_{2(g)} \tag{6}$$

$$Cl_{2(g)} + Hg_{(g)} \rightarrow HgCl_{2(g)} \tag{7}$$
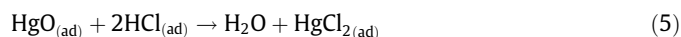
4. Conclusions

Ag doped can significantly improve the performance of the SCR catalyst, especially at low temperatures. Ag was present with a mixture of zero-oxidation silver (Ag^0) and Ag^+ (Ag_2O), and the metallic state was mostly existence. In addition, Agcan keep the elements of V, Mo and Ti in their higher oxidation states, and it could weak the bond strength of V=O and Mo=O and decrease the activation energy values of desorption of surface oxygen species. Therefore, it increases the oxidation ability of catalyst and lower the redox temperature. The Hg^0 catalytic oxidation results indicated that the catalyst of Ag-V-Mo-Ti had a highest catalytic efficiency and a wide temperature window. The influence of SO_2 was inhibited and NO was promoted, while water inhibited slightly at low temperature and promoted slightly at high temperature. The catalytic mechanism was that adsorbed Cl reacted with the Hg^0 both adsorbed on the support and the silver amalgam at low temperature. However, adsorbed active chlorine atoms reacted with gaseous mercury at middle temperature, and Cl and Cl_2 reacted with Hg^0 over the direct gas phase oxidation at high temperature. These above mentioned were all beneficial for the oxidation of mercury.
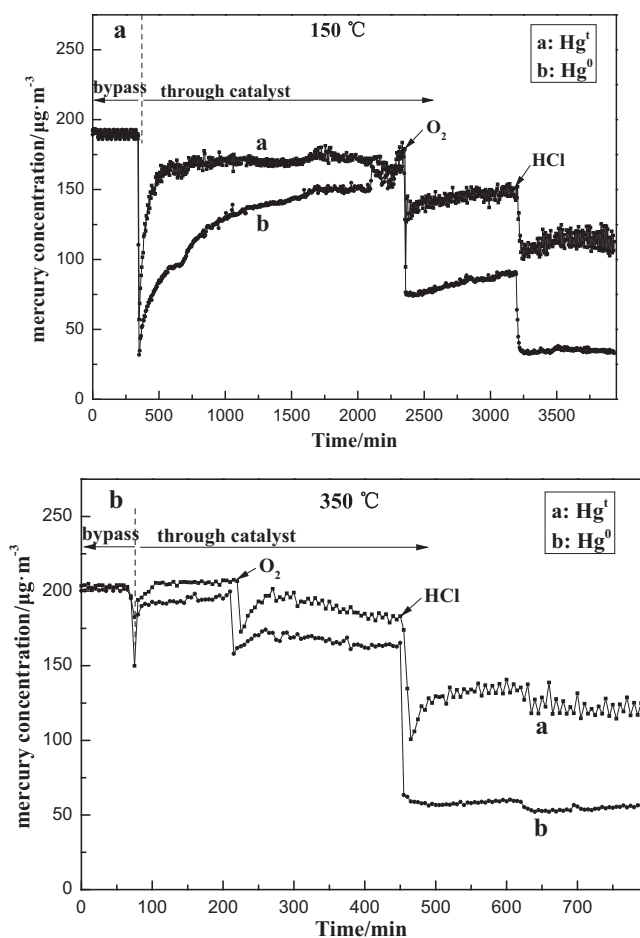
Fig. 4. Mercury concentration change curves: 150 °C (a), 350 °C (b).
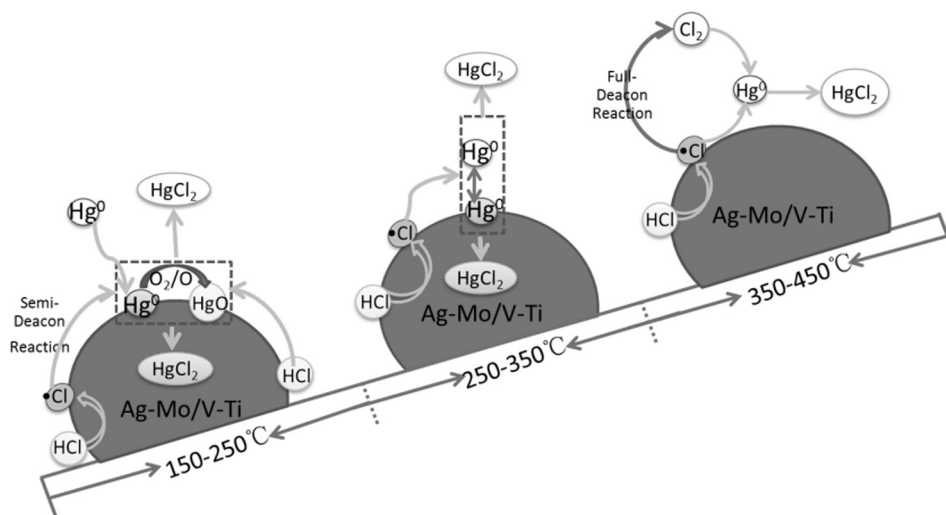
Fig. 5. The reaction process for the Hg^0 oxidation over Ag-Mo/V-Ti at various temperature ranges.

Acknowledgements

Appendix A. Supplementary data

Supplementary data associated with this article can be found, in the online version, at http://dx.doi.org/10.1016/j.fuel.2017.03.034.

References

[1] Kamata H, Yukimura A. Catalyst aging in a coal combustion flue gas for mercury oxidation. Fuel Process Technol 2012;104:295–9.

[2] Pavlish JH, Sondreal EA, Mann MD, Olson ES, Galbreath KC, Laudal DL, et al. Status review of mercury control options for coal-fired power plants. Fuel Process Technol 2003;82:89–165.

[3] U.S. Environmental Protection Agency Air toxics standards for utilities. In: <http://www.epa.gov/airquality/powerplanttoxics/actions.html>.

[4] Gao W, Liu Q, Wu CY, Li H, Li Y, Yang J, et al. Kinetics of mercury oxidation in the presence of hydrochloric acid and oxygen over a commercial SCR catalyst. Chem Eng J 2013;220:53–60.

[5] Uddin MA, Yamada T, Ochiai R, Sasaoka E, Wu S. Role of SO_2 for elemental mercury removal from coal combustion flue gas by activated carbon. Energy Fuels 2008;22:2284–9.

[6] Senior CL, Helble JJ, Sarofim AF. Emissions of mercury, trace elements, and fine particles from stationary combustion sources. Fuel Process Technol 2000;65:263–88.

[7] Presto AA, Granite EJ. Survey of catalysts for oxidation of mercury in flue gas. Environ Sci Technol 2006;40:5601–9.

[8] Eom Y, Jeon SH, Ngo TA, Kim J, Lee TG. Heterogeneous mercury reaction on a selective catalytic reduction (SCR) catalyst. Catal Lett 2008;121:219–25.

[9] Kamata H, Ueno S, Naito T, Yukimura A. Mercury oxidation over the V_2O_5 (WO_3)/TiO_2 commercial SCR catalyst. Ind Eng Chem Res 2008;47:8136–41.

[10] Giamello E. Characterization and reactivity of V_2O_5-MoO_3/TiO_2 de-NOx SCR catalysts. J Catal 1999;187:419–35.

[11] Li H, Li Y, Wu CY, Zhang J. Oxidation and capture of elemental mercury over SiO_2-TiO_2-V_2O_5 catalysts in simulated low-rank coal combustion flue gas. Chem Eng J 2011;169:186–93.

[12] Kornelak P, Mizukami F, Weselucha-Birczyńska A, Proniewicz L, Djega-Mariadassou G, Białas A, et al. Evolution of active species of nanostructured anatase-supported V-O–Mo catalyst in the course of reduction and oxidation. Catal Today 2004;90:103–7.

[13] Matralis H, Papadopoulou C, Kordulis C, Aguilar Elguezabal A, Cortes Corberan V. Selective oxidation of toluene over V_2O_5/TiO_2 catalysts. Effect of vanadium loading and of molybdenum addition on the catalytic properties. Appl Catal A 1995;126:365–80.

[14] Bertinchamps F, Treinen M, Eloy P, Dos Santos A, Mestdagh M, Gaigneaux E. Understanding the activation mechanism induced by NOx on the performances of VOx/TiO_2 based catalysts in the total oxidation of chlorinated VOCs. Appl Catal B 2007;70:360–9.

[15] Lee CW, Serre SD, Zhao Y, Lee SJ, Hastings TW. Mercury oxidation promoted by a selective catalytic reduction catalyst under simulated powder river basin coal combustion conditions. J Air Waste Manage Assoc 2008;58: 484–93.

[16] Yang X, Ma FY, Li KX, Guo YG, Hu JL, Li W, et al. Mixed phase titania nanocomposite codoped with metallic silver and vanadium oxide: new efficient photocatalyst for dye degradation. J Hazard Mater 2010;175: 429–38.

[17] Yeom YH, Li MJ, Sachtler WMH, Weitz E. Low-temperature NOx reduction with ethanol over Ag/Y: a comparison with Ag/gamma-Al_2O_3 and BaNa/Y. J Catal 2007;246:413–27.

[18] Satokawa S, Shibata J, Shimizu KI, Satsuma A, Hattori T. KojimaT. Promotion effect of hydrogen on lean NO, reduction by hydrocarbons over Ag/Al(2)O (3)catalyst. Chem Eng Sci 2007;62:5335–7.

[19] Delaigle R, Eloy P, Gaigneaux E. Necessary conditions for a synergy between Ag and V_2O_5 in the total oxidation of chlorobenzene. Catal Today 2011;175:177–82.

[20] Ge X, Zhang HL. Temperature-programmed reduction studies of V-Ag catalysts. J Solid State Chem 1998;141:186–90.

[21] Yuan Y, Zhao Y, Li H, Li Y, Gao X, Zheng C, et al. Electrospun metal oxide–TiO_2 nanofibers for elemental mercury removal from flue gas. J Hazard Mater 2012;227:427–35.

[22] Dong J, Xu Z, Kuznicki SM. Mercury removal from flue gases by novel regenerable magnetic nanocomposite sorbents. Environ Sci Technol 2009;43:3266–71.

[23] Zhang Y, Tang ZR, Fu X, Xu YJ. Nanocomposite of Ag–AgBr–TiO_2 as a photoactive and durable catalyst for degradation of volatile organic compounds in the gas phase. Appl Catal B 2011;106:445–52.

[24] Cheng XW, Yu XJ, Li BY, Yan L, Xing ZP, Li JJ. Enhanced visible light activity and mechanism of TiO_2 codoped with molybdenum and nitrogen. Mater Sci Eng B 2013;178:425–30.

[25] Atla SB, Chen CC, Chen CY, Lin PY, Pan W, Cheng KC, et al. Visible light response of Ag^+/TiO_2-Ti_2O_3 prepared by photodeposition under foam fractionation. J Photochem Photobiol A 2012;236:1–8.

[26] Neophytides S, Zafeiratos S, Kennou S. XPS characterization of the electrochemically generated O species on a Au electrode evaporated on Y_2O_3-stabilized ZrO_2 (100). Solid State Ionics 2000;136:801–6.

[27] Jung JI, Edwards DD. X-ray photoelectron (XPS) and Diffuse Reflectance Infra Fourier Transformation (DRIFT) study of $Ba_{0.5}Sr_{0.5}Co_xFe_{1-x}O_3$-delta (BSCF: x=0-0.8) ceramics. J Solid State Chem 2011;184:2238–43.

[28] Savinova ER, Scheybal A, Danckwerts M, Wild U, Pettinger B, Doblhofer K, et al. Structure and dynamics of the interface between a Ag single crystal electrode and an aqueous electrolyte. Faraday Discuss 2002;121:181–98.

[29] Kaichev V, Bukhtiyarov V, Hävecker M, Knop-Gercke A, Mayer R, Schlögl R. The nature of electrophilic and nucleophilic oxygen adsorbed on silver. Kinet Catal 2003;44:432–40.

[30] Hu Y, Lü W, Liu D, Liu J, Shi L, Sun Q. Effect of ZnO on the performance of Ag/ SiO_2 catalyst for the vapor-phase synthesis of 3-methylindole. J Nat Gas Chem 2009;18:445–8.

[31] Zaihua W, Xinjun L, Wenji S, Jinfa C, Tao L, Ziping F. Promotional effect of Ag-doped Ag–V/TiO_2 catalyst with low vanadium loadings for selective catalytic reduction of NO_X by NH_3. React Kinet Mech Catal 2011;103:353–65.

[32] Xue M, Ge J, Zhang H, Shen J. Surface acidic and redox properties of V-Ag-Ni-O catalysts for the selective oxidation of toluene to benzaldehyde. Appl Catal A 2007;330:117–26.

[33] Yang S, Iglesia E, Bell AT. Oxidative dehydrogenation of propane over V_2O_5/MoO_3/Al_2O_3 and V_2O_5/Cr_2O_3/Al_2O_3: structural characterization and catalytic function. J Phys Chem B 2005;109:8987–9000.

[34] Meischen SJ, Van Pelt VJ. Method to control mercury emissions from exhaust gases. In: Google Patents; 2000.

[35] Luo G, Yao H, Xu M, Cui X, Chen W, Gupta R, et al. Carbon nanotube-silver composite for mercury capture and analysis. Energy Fuels 2009;24:419–26.

[36] Li H, Wu CY, Li Y, Zhang J. CeO_2–TiO_2 catalysts for catalytic oxidation of elemental mercury in low-rank coal combustion flue gas. Environ Sci Technol 2011;45:7394–400.

[37] Yan NQ, Chen WM, Chen J, Qu Z, Guo YF, Yang SJ, et al. Significance of RuO_2 modified SCR catalyst for elemental mercury oxidation in coal-fired flue gas. Environ Sci Technol 2011;45:5725–30.

[38] Li Y, Murphy PD, Wu CY, Powers KW, Bonzongo JC. Development of silica/vanadia/titania catalysts for removal of elemental mercury from coal-combustion flue gas. Environ Sci Technol 2008;42:5304–9.